Title: Scalable production of large quantities of defect-free, few-layer graphene by shear exfoliation in liquids

Authors: Keith R Paton[1,2], Eswaraiah Varrla[1,3], Claudia Backes[1,3], Ronan J Smith[1,3], Umar Khan[1,3], Arlene O'Neill[1,3], Conor Boland[1,3], Mustafa Lotya[1,3], Oana M Istrate[1,3], Paul King[1,3], Tom Higgins[1,3], Sebastian Barwich[1,3], Peter May[1,3], Pawel Puczkarski[1,3], Iftikhar Ahmed[4], Matthias Moebius[3], Henrik Pettersson[1,3], Edmund Long[1,3], João Coelho[1,4], Sean E O'Brien[1,3], Eva K McGuire[1,3], Beatriz Mendoza Sanchez[1,4], Georg S Duesberg[1,4], Niall McEvoy[1,4], Timothy J. Pennycook[5], Clive Downing[1], Alison Crossley[6], Valeria Nicolosi[1,3,4] and Jonathan N Coleman[1,3]*

Affiliations:

[1]Centre for Research on Adaptive Nanostructures and Nanodevices (CRANN), Trinity College Dublin, Dublin 2, Ireland.

[2]Thomas Swan & Co. Ltd., Rotary Way, Consett, County Durham, DH8 7ND, United Kingdom.

[3]School of Physics, Trinity College Dublin, Dublin 2, Ireland.

[4]School of Chemistry, Trinity College Dublin, Dublin 2, Ireland.

[5]SuperSTEM, STFC Daresbury Laboratories, Keckwick Lane, Warrington,WA4 4AD United Kingdom.

[6]Department of Materials, University of Oxford, Parks Road, OX1 3PH, Oxford, United Kingdom.

*Correspondence to: colemaj@tcd.ie.

Abstract: In order to progress from the lab to commercial applications it will be necessary to develop industrially scalable methods to produce large quantities of defect-free graphene. Here we show that high-shear mixing of graphite in suitable, stabilizing liquids results in large-scale exfoliation to give dispersions of graphene nanosheets. XPS and Raman spectroscopy show the exfoliated flakes to be unoxidised and free of basal plane defects. We have developed a simple model which shows exfoliation to occur once the local shear rate exceeds 10^4 s^{-1}. By fully characterizing the scaling behaviour of the graphene production rate, we show that exfoliation can be achieved in liquid volumes from 100s of ml up to 100s of litres and beyond. The graphene produced by this method performs well in applications from composites to conductive coatings. This method can be applied to exfoliate BN, MoS_2 and a range of other layered crystals.

Main Text:

Due to its ultra-thin, 2-dimensional nature and its unprecedented combination of physical properties, graphene has become the most studied of all nano-materials. In the next decade graphene is likely to find commercial applications in many areas from high-frequency electronics to smart coatings.[1] Some important classes of applications, such as printed electronics, conductive coatings and composite fillers, will require industrial-scale production of defect-free graphene in a processable form. For example, graphene is likely to be used as a low-cost electrode material in applications such as solar cells,[2] batteries[3] and sensors[4]. Such electrodes will almost certainly be produced by solution-coating and so will require large quantities of graphene in the form of liquid suspensions, inks or dispersions[1]. Thus, liquid exfoliation of graphene will become a critically important technology in the near future.[5,6] However, no scalable method exists to give large quantities of graphene that is *also* defect-free. For example, while oxidative exfoliation of graphite can potentially give large quantities

of graphene-like nanosheets, such graphene-oxide is typically defective.[7] Although, graphene-oxide has proven very useful in applications from composites to catalysis,[8,9] it is very likely that an equally wide range of applications will require graphene that is free of basal-plane defects. Alternatively, sonication of graphite,[10] or indeed other layered compounds,[11] in certain stabilising solvents or aqueous surfactant solutions[12,13] gives defect-free nanosheets. However, the scalability of the latter process is limited by the use of sonication as an energy source.

Thus, solution- exfoliation methods tend to display either high production rates or low defect contents, but not both. A detailed literature survey[14] shows that no papers describe production rates above 0.4 g/h coupled with Raman D:G intensity ratios (a measure of defect content) below 0.65. In fact 80% of the papers surveyed had production rates below 0.04 g/h,[14] far too low for commercial production. One possible solution would be to find a scalable method of exfoliation which, coupled with the use of stabilising liquids, could lead to large scale graphene production.

Here, we demonstrate high-shear mixing[14] as a scalable alternative to sonication for the exfoliation of layered crystals such as graphite. Shear mixing is already widely used to disperse nanoparticles in liquids. However, in general this involves breaking up of nanoparticle agglomerates[15] which are very weakly bound compared to the inter-sheet binding strength in graphite. A number of papers and patents have described methods for the exfoliation of graphite or layered compounds that incorporate shear mixing as part of the process. However, in such cases, the layered crystal was first swelled by intercalation, significantly weakening the inter-layer binding strength.[16-19] Under these circumstances, shear mixing can be used to exfoliate the crystal to give dispersed nanosheets. However, such methodologies just shift the rate-limiting step from exfoliation to intercalation, limiting the potential for scale-up. What would be more useful would be if untreated layered crystals

could be exfoliated in liquids using only shear mixing. This would allow the application of the well-known strategies for the scale-up of shear mixing processes that are commonly used in industry.[20] However, at first glance shear mixing alone seems an unlikely candidate for exfoliation of layered crystals. When using ultrasonic probes to exfoliate graphite, energy densities of thousands of W/L are typically used.[21] Lab-scale shear mixers typically deliver 100s of W into a few litres of liquid resulting in powder densities of ~100 W/L. Thus, one would expect exfoliation under shear to either not occur at all or to proceed at a much lower rate than sonication-induced exfoliation. However, a recent paper has shown that graphite can be exfoliated to give graphene by generating shear in a very thin liquid layer in a rapidly rotating tube.[22] However, this method gives very small quantities of graphene and is inherently un-scalable. Here we demonstrate a method for shear-exfoliation of graphite to give graphene that is many times more efficient than sonication but which can be scaled-up to an industrial level. We show that shear exfoliation can produce large quantities of defect-free, unoxidised graphene and develop a model that quantitatively describes the process. In addition, this graphene performs very well in a range of applications and this method can be used to exfoliate numerous other layered crystals.

Shown in figure 1A is a Silverson model L5M mixer that generates high shear using a closely spaced (~120 μm) rotor/stator combination (figure 1B), and is available with a range of rotor diameters (figure 1B-C). Initial shear-mixing trials[14] exfoliated graphite both in the solvent N-methyl-2-pyrrolidone (NMP) and in aqueous surfactant solutions (sodium cholate, NaC),[10] to give large-volume suspensions (figure 1D, processing parameters: rotor diameter, D=32 mm; initial graphite concentration, C_i=50 mg/ml; mixing time, t=20 min; liquid volume, V=4.5 L; rotor speed, N=4500 rpm). After centrifugation (1500 rpm, 150 minutes) these suspensions contain large quantities of high quality graphene nanosheets, including some monolayers (figure 1E-H).

To test the effect of mixing parameters on the quality of shear-exfoliated graphene (SEG), we prepared a range of dispersions using both NMP and water/NaC, keeping all but one of the mixing parameters constant (see above) but maximising and minimising the remaining one.[14] These dispersions were studied by TEM and AFM to measure the flake size and thickness before filtering to form ~100 nm thick films which were characterised by XPS and Raman spectroscopy (figure 1 I-K).[14] TEM measurements showed nanosheet sizes in the 300-800 nm range while AFM gave typical thicknesses, N_G, of less than 10 monolayers per nanosheet ($\langle N_G \rangle$~5-8).[14] The presence of monolayers was confirmed by Raman spectroscopy (figure 1I, inset). For the films XPS showed no evidence of oxidation while Raman spectroscopy reproducably showed a 2D band consistent with few-layer graphene (inset) and a relatively weak, narrow D-band.[14] The Raman D:G band intensity ratio is proportional to inverse nanosheet length[23] while the D:D' band intensity ratio[24] is ~4.[14] Taken together, these data show the D band to be dominated by nanosheet edge contributions and confirms that no basal plane defects are introduced during exfoliation.[14,23,24] As shown in figure 1L, these properties were relatively invariant with mixing parameters indicating that well exfoliated, non-oxidised, defect-free graphene can be produced using a broad range of mixing conditions. We note that these flakes are virtually indistinguishable from those produced by sonication both in terms of size and quality.[10]

Considering the exfoliation mechanism, our initial expectation was that localized, turbulent, highly-dissipative regions were responsible for exfoliation.[25,26] However, we found turbulent energy dissipation to be unnecessary. Figure 2A maps the combinations of N and D that result in exfoliation: graphene is produced not only for turbulent, high Reynolds number (Re) scenarios, but also for combinations which give $\mathrm{Re}_{Mixer} = ND^2\rho/\eta < 10^4$, where turbulence is not fully developed.[27] To see if graphene could be produced in the complete absence of turbulence, i.e. under high-shear laminar flow, we mixed graphene in a Couette (a concentric

cylinder-based rheological cell, radius R=14 mm, thickness d=0.1 mm, rotation frequency of inner wall ω: shear rate $\dot{\gamma} \approx R\omega / d$).[14] TEM confirmed graphene was produced, with concentration increasing with time as $t^{0.69}$ (figure 2B). Interestingly, we found graphene in the Couette only above a minimum shear rate of $\dot{\gamma}_{min} \approx 10^4$ s^{-1} (figure 2C). However, this rate is low enough to give a Reynolds number well within the laminar flow regime ($\dot{\gamma}_{min} = 10^4$ s^{-1}: $\mathrm{Re}_{Couette} = \dot{\gamma} d^2 \rho / \eta = 60$)[28] showing turbulence to be unnecessary for exfoliation.

To see if a minimum shear rate is a general requirement; we prepared graphene in the shear mixer at a number of different N and D combinations. The concentration produced after 1 minute's mixing, $C_{1\,min}$, is plotted against the shear rate ($\dot{\gamma} \approx \pi ND / \Delta R$ where ΔR is the rotor/stator gap) in figure 2D. This shows a minimum shear rate of $\dot{\gamma}_{min} \approx 10^4$ s^{-1}, implying that the same exfoliation mechanism occurs in both laminar and turbulent regimes. We note that all the well-exfoliated samples in figure 2A are consistent with $\dot{\gamma}_{min} > 10^4$ s^{-1}. This suggests that any mixer which can achieve this shear rate can be used to produce graphene. We demonstrate this to be true by using a Kenwood kitchen blender to exfoliate graphite to give graphene. Here, exfoliation occurs because the rapidly rotating blade generates local turbulent shear rates significantly larger than 10^4 s^{-1}.[14]

We can understand these processes by modelling exfoliation as shear-induced inter-monolayer sliding in a solvent.[14,22] This predicts a minimum shear rate given by:

$$\dot{\gamma}_{min} = \frac{\left[\sqrt{E_{S,G}} - \sqrt{E_{S,L}}\right]^2}{\eta L} \qquad (1)$$

where $E_{S,G}$ and $E_{S,L}$ are the surface energies of graphene and liquid ($E_{S,L}$=69 mJ/m^2 for NMP[10]), η is the liquid viscosity (0.0017 Pa·s for NMP) and L is the flake length. This equation clearly shows the role of the solvent: for solvents with surface energies matching

graphene, the exfoliation energy is minimised, facilitating shear exfoliation at low shear rates. Given the flake size measured by TEM (~300-800 nm) and $\dot{\gamma}_{min}$ =10^4 s^{-1}, equation 1 predicts $E_{S,G}$≈70.5-71 mJ/m^2, close to the expected value.[10]

Equation 1 can be rewritten to express the minimum flake size that can be produced by shear exfoliation at a given $\dot{\gamma}$.[14] Then, the average flake size, $\langle L \rangle$, is approximately the mean of this value and the maximum flake size retained after centrifugation, L_{CF}. Writing in terms of N and D rather than $\dot{\gamma}$:

$$\langle L \rangle \approx \frac{\Delta R\left[\sqrt{E_{S,G}} - \sqrt{E_{S,L}}\right]^2}{2\eta\pi ND} + \frac{L_{CF}}{2} \qquad (2)$$

Shown in figure 2E is data for mean flake length measured by TEM[14] as a function of N. Equation 2 fits the data extremely well and gives $E_{S,G}$≈70.6 mJ/m^2 and L_{CF}=900 nm, close to expected values[14]. We note that this expression also fits the data for L as a function of D.[14]

This mechanism is general and does not only apply to graphite. In fact we were able to exfoliate BN, WS_2, $MoSe_2$, $MoTe_2$ in NMP using this mixer (see SI and below).[14] Shown in figure 2F is a TEM image of a partially exfoliated BN flake displaying laterally displaced monolayers consistent with the proposed shear-exfoliation method.[22]

It is important to understand what controls the amount of graphene produced with the aim of maximising the production rate by scale-up. As properties of shear-mixed dispersions tend to scale with processing parameters as power laws,[14,29,30] the graphene concentration should scale as

$$C \propto C_i^{\chi} t^{\tau} N^n D^d V^v \qquad (3)$$

To test this, we prepared a wide range of dispersions, controllably varying all five mixing parameters. These were centrifuged and the graphene concentration measured optically.[14]

Keeping C_i, N, D and V constant but varying t showed $C \propto t^{\tau}$ where τ is close to 0.66 (figure 3A), very similar to the Couette exponent.[14] We note that sonication-exfoliation of graphene in solvents gives $C \propto t^{1/2}$,[23] suggesting that time exponents close to 0.5-0.7 may be process-independent and so represent more fundamental behaviour.

In some cases, C saturated for times above a maximum value, t_{sat}, setting a maximum mixing time. We found t_{sat} to be proportional to $VN^{-1}D^{-3}$ (figure 3B), a quantity related to the time for the tank volume to be pumped through the rotor/stator once.[31] Measurements of C *versus* t allowed the calculation of a representative concentration *e.g.* that achieved after 1 minute mixing, $C_{1\ min}$. Measurements of $C_{1\ min}$ for different combinations of C_i, D, N and V (figure 3 C-F) showed that power-law behaviour was observed with exponents: χ=1.0, d=2.28, ν=-0.68. When varying N, power-law behaviour (n=1.13) was only observed above a minimum rpm, N_{min}, which is associated with the minimum shear rate described above.

Because of these scaling laws, the concentration data should fall on a master-curve when plotted against the scaling factor $C_i t^{0.66} N^{1.13} D^{2.28} V^{-0.68}$, as confirmed in figure 4A. These exponents are not specific to graphene; we plotted the concentration of MoS_2 exfoliated in NMP *versus* $C_i t^{0.66} N^{1.13} D^{2.28} V^{-0.68}$ (i.e. using same exponents as graphene in NMP) finding reasonable linearity (figure 4B).

Studies on the breakage of ceramic materials in rotor stator mixers have suggested a link between particle concentration and total energy dissipated per volume.[32,33] The power dissipated by a rotor/stator mixer is given by $P = N_P \rho N^3 D^5$ where ρ is the solvent density and $N_P \approx 2$.[27,29] This expression, coupled with the exponents measured for mixing in NMP suggest equation 3 to be approximately equivalent to $Y = C / C_i \propto \sqrt{E/V}$ where Y is the graphene yield and E/V is the total energy dissipated per unit volume.[14] Plotting Y *versus*

E/V confirms this to be approximately true (figure 4C). This allows us to compare shear exfoliation to sonication-induced exfoliation (figure 4C), showing shear exfoliation to be considerably more efficient than ultrasonic exfoliation, becoming more so as the volume is increased.[14] In addition to its inherent scalability, this result shows that shear exfoliation gives much larger quantities of graphene at lower energy cost than is possible with sonication-induced exfoliation. It is worth noting that the exfoliation yields are relatively low at <0.1%. However, by recycling graphitic sediment at least 3% of the graphite can be transformed into graphene.[14] Moreover, the yield might be enhanced dramatically by careful choice of the starting graphite material.

For commercial production, the most important parameter is the graphene production rate: $P_R = VC/t$. Figure 4D demonstrates a master curve of production rate plotted *versus* the scaling factor $C_i t^{\tau-1} N^n D^d V^{v+1}$ with exponents as above. The maximum production rate achieved in lab trials was 1.44 g/h (for short mixing times), far higher than any rate previously achieved for solution processed defect-free graphene.[14]

It will be more straightforward to scaleup shear exfoliation of graphene in aqueous rather than organic solvent environments. Thus, for large-scale studies, we focused on exfoliation by mixing in aqueous solutions of the surfactant sodium cholate (although polymers such as polyvinylalcohol can also be used).[14] For both polymer- and surfactant-stabilised graphene, scaling behaviour was found[14] with the data for graphene exfoliated in sodium cholate shown in figure 4E. Here the scaling exponents are slightly different with $C \propto C_i t^{1.08} N^{2.54} D^{3.34} V^{-0.47}$, possibly reflecting mechanistic differences.

On scale-up, the mixing time should be fixed at $t_{sat} \propto VN^{-1}D^{-3}$, while the rotor/stator diameter should be scaled in proportion to tank size ($D \propto V^{1/3}$).[14] This predicts $P_R \propto V^{v+1+d/3}$,

giving $P_R \propto V^{1.1}$ for NMP and $P_R \propto V^{1.6}$ for surfactant, confirming that production rate can be increased by scaling up the mixing volume. We performed large scale trials (figure 4 F-H), mixing in surfactant solution (C_i=100 mg/ml, t=5 min-4 h, N=3000 rpm, D=11 cm), with volumes up to V=300 L.[14] This yielded up to 21 g of high quality graphene (Raman ratio of 0.18) per batch with concentrations up to C=0.07 mg/ml and production rates as high as P_R=5.3 g/h, significantly better than any reported work.[14] Both lab-scale and large-scale concentration data followed the same scaling law (figure 4E). This allows us to estimate that on scale-up to V=10 m^3, production rates exceeding 100 g/h are possible.[14] A detailed literature review shows that no report comes close to the combination of high production rate, low Raman D:G ratio and lack of oxides reported here.[14]

The SEG produced has been tested in a range of applications that require large quantities of cheap, yet good-quality graphene.[14] The most obvious application is reinforcement of melt-processed composites. We added 0.07 wt% graphene to PET, a common engineering plastic, by melt mixing resulting in macroscopic composites (figure 5A) with well-dispersed graphene nanosheets (figure 5B). At this loading level, we found a 40% increase in strength and a 13% increase in modulus (figure 5C), a level of reinforcement which far surpasses that found for any other filler.[14] We produced thin films of graphene nanosheets (figure 5D) which have conductivity as high as 400 S/cm (figure 5E), competitive with other solution-processed graphenes[34] and suitable for electrode applications. One example is the replacement of the Pt/ITO electrodes in a dye-sensitised solar cell, resulting in similar levels of efficiency (figure 5F). Thin films (25 nm) of SEG display a combination of high electrolytic capacitance at 120 Hz and phase angle close to 90^o (figure 5G-H) suitable for use as micro-supercapacitors in electronic smoothing applications.[35] This capacitance is 10^6 times higher than nanostructured dielectric capacitors[36] and is competitive with much thicker electrodes of existing materials.[37] We have also produced novel composites by soaking

commercially available elastic bands in dispersions of SEG in NMP resulting in infusion of graphene into the surface of the elastomer. This renders the band conductive with a resistance that depends exponentially on strain. Such bands make very effective dynamic strain sensors with low-strain gauge factors of ~8 and effective strain range of up to 300%, far superior to commercial metal strain gauges (figure 5 I-J).[38]

Acknowledgements: We thank Science Foundation Ireland, the European Research Council, the Graphene Flagship Project and Thomas Swan for financial support. We acknowledge the CRANN Advanced Microscopy Lab for technical support.

Author contributions: KRP, EV & PP performed the shear mixing and other experiments. AO'N, ML, PM, RJS, HP, EL, JC, SEO'B, BMS, EMcG, TJP, VN performed electron microscopy characterization and analysis. CD and AC performed XPS characterization and analysis. UK, CB, OMI, PK, TH, IA performed applications measurements. CB, N McE & GSD performed Raman and AFM analysis. SB and MM performed rheological characterization and analysis. JNC designed the experiments, derived the models and wrote the paper.

Competing financial interests: None

Figures

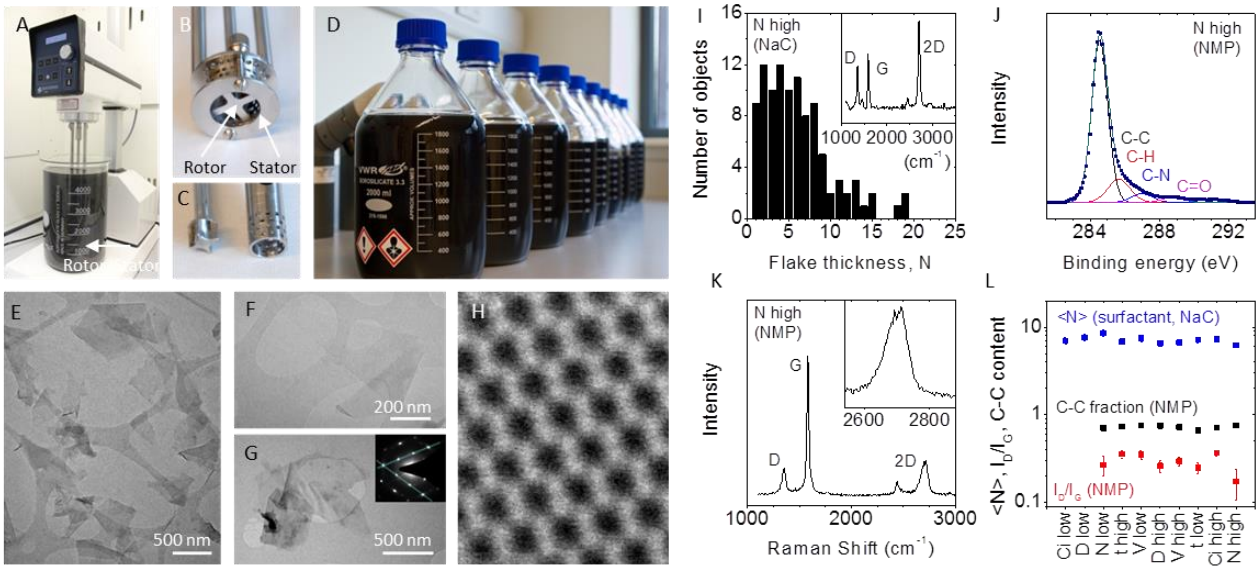

Figure 1: Production of graphene by shear mixing. A) A Silverson model L5M high-shear mixer with mixing head in a 5L beaker of graphene dispersion. B-C) Close-up view of B) a D=32 mm mixing head and C) a D=16 mm mixing head with rotor (left) separated from stator. D) Graphene-NMP dispersions produced by shear exfoliation. E) Wide-field TEM image of shear-exfoliated graphene nanosheets (after centrifugation). F-H) TEM images of F) an individual nanosheet, G) a multilayer (bottom left) and monolayer (right) as evidenced by its electron diffraction pattern (inset) and H) a monolayer (imaged by high resolution scanning TEM). I) Histogram of nanosheet thickness as measured by AFM on a surfactant exfoliated sample. The presence of monolayers was confirmed by Raman characterisation (inset). J-K) XPS and Raman spectra (NMP exfoliated samples) measured on thin films. AFM, Raman and XPS analysis was performed on dispersions made using both high and low values of a given processing parameter while keeping others constant[14]. The dispersion type is indicated in the panel. L) Information extracted from Raman, XPS and flake thickness data plotted *versus* dispersion type. Blue – mean flake thickness measured for a surfactant exfoliated dispersion, <N>; black – fraction of XPS spectrum associated with C-C bonds; red

– ratio of intensities of Raman D and G bands. Unless noted otherwise, all data is reported for NMP dispersions.

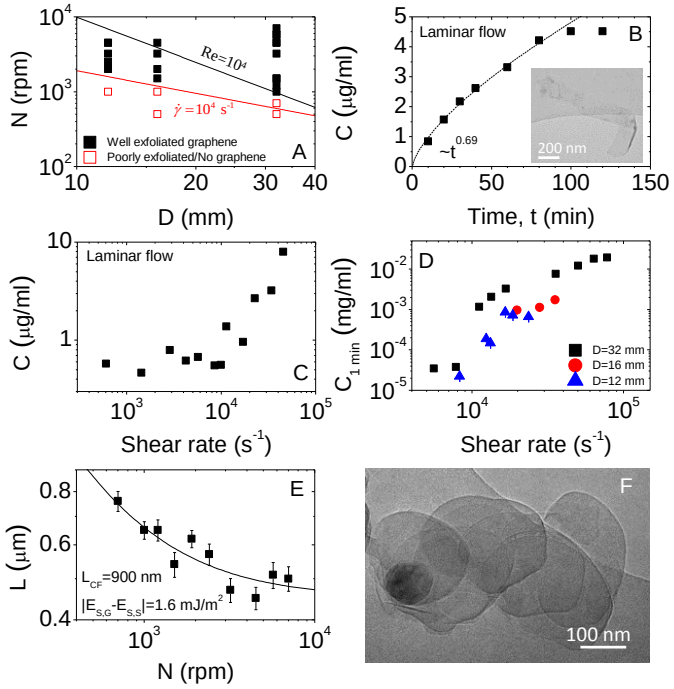

Figure 2: Characterisation of the exfoliation mechanism. A) Phase diagram of rotor speed, N, *versus* diameter, D, for dispersions showing good exfoliation according to TEM. The region above the solid line represents fully developed turbulence i.e. Re>10^4 while the region above the red line represents $\dot{\gamma}_{min}$ >10^4 s^{-1}. B) Concentration (after CF) of graphene produced in a rotating Couette as a function of mixing time (rotation rate 3000 rpm). Inset: TEM of Couette produced graphene. C) Concentration (after CF) of graphene produced in a rotating Couette as a function of shear rate (mixing time 60 min). D) Concentration of graphene produced in a shear mixer as a function of shear rate for rotors with diameters of 32, 16 and 12 mm (mixing time 1 min). All three data sets are consistent with the same minimum shear rate. E) Mean flake length plotted *versus* rotor speed, N (C_i=50 mg/ml; t=20 min; V=4.5 L; D=32 mm). The solid line is a fit to equation 3. F) TEM image of partially exfoliated BN flake, consistent with exfoliation by shear sliding.

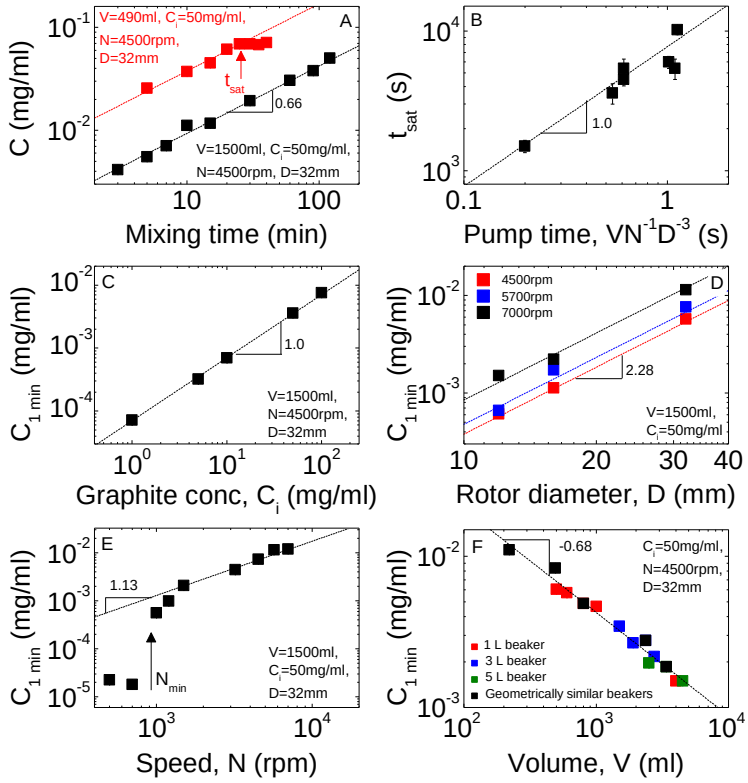

Figure 3: Scaling of graphene production using a shear mixer. A) Dispersed concentration, C, (after centrifugation) plotted as a function of mixing time, t. The lines denote behaviour of the type: $C \propto t^{\tau}$ where τ is always close to 0.66. B) Graph of the measured values of saturation time, t_{sat}, plotted *versus* pumping time $VN^{-1}D^{-3}$. C-F) Values of graphene concentration after 1 minute of mixing, $C_{1\ min}$, plotted against C) initial graphite concentration, C_i; D) rotor diameter, D; E) mixing speed, N and F) liquid volume, V. In C-F) the mixing parameters are given in the panels. The minimum required mixing speed, N_{min}, is indicated by the arrow. In F), a number of beakers of different capacity, holding a range of liquid volumes were used.[14] Geometrically similar denotes beakers holding a specific liquid volume such that the liquid height was equal to the beaker diameter.

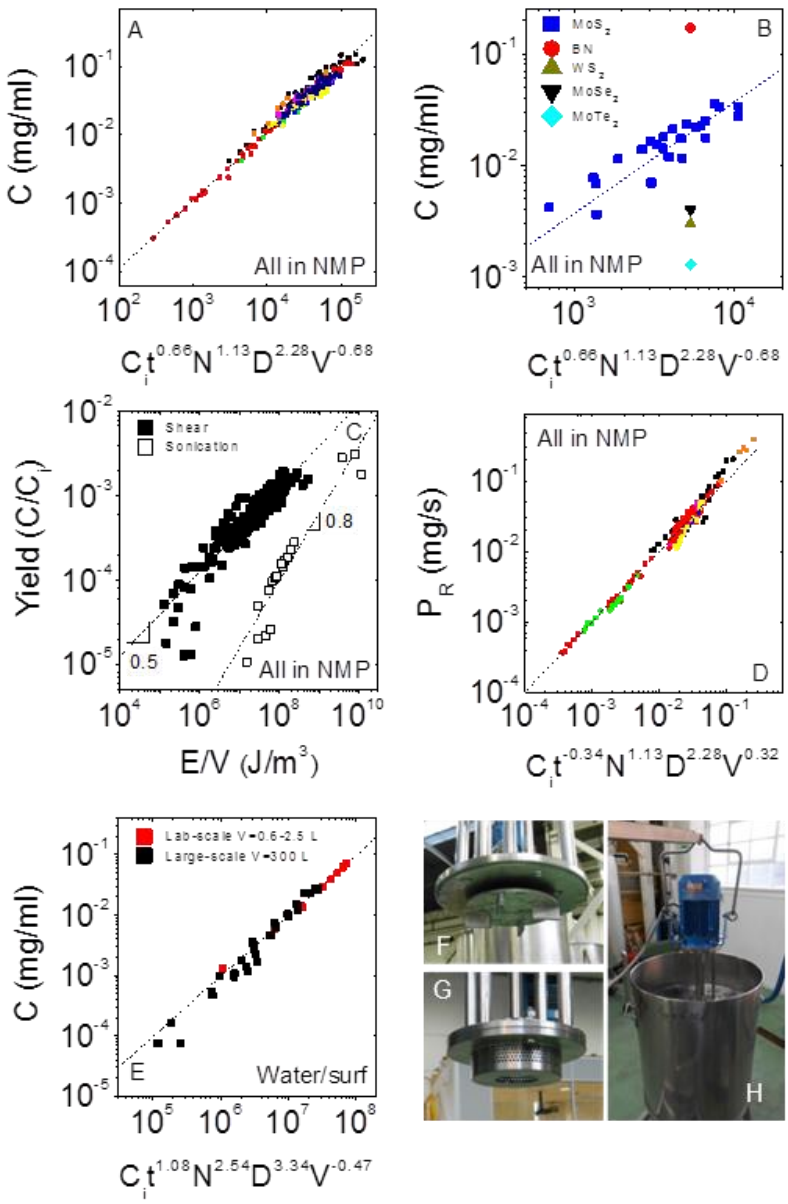

Figure 4: Scaling of graphene production using a shear mixer. A) Graphene concentration in NMP plotted against a composite variable indicating that all data follows the scaling laws discussed in the text. B) Post CF concentration of MoS_2 in NMP, plotted against a composite variable indicating that all data follow the scaling laws discussed in the text. Also shown in B) are results of single trials to exfoliate BN, WS_2, $MoSe_2$ and $MoTe_2$, all in NMP. C) Graphene yield measured *versus* energy density. Also shown is equivalent data for horn-sonicated graphite (t=15-360 min, V=0.22-1 L, delivered power~20 W). D) Graphene

production rate in NMP plotted against the appropriate composite variable. E) Concentration of surfactant-exfoliated graphene plotted against a composite variable. F-H) Ten cm diameter F) rotor and G) stator used during large scale trials. H) Shear exfoliation of graphite in water-surfactant solution at the V=100 L scale.

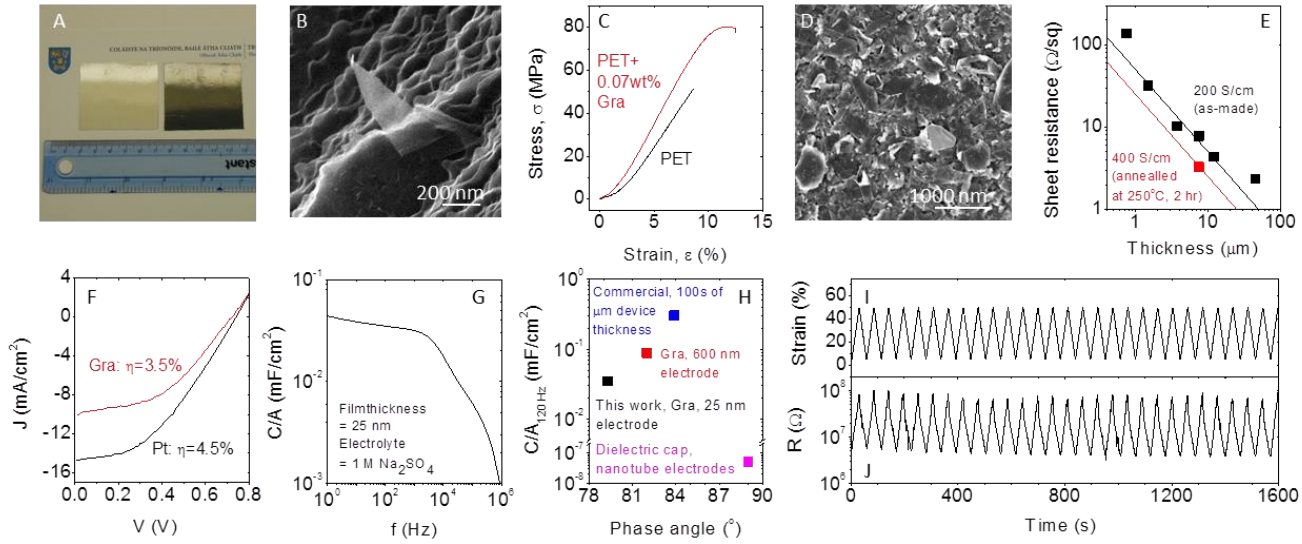

Figure 5: Applications of mixer exfoliated graphene. A) Melt-processed pieces of (left) PET and (right) PET:Graphene-0.07%. B) Helium ion micrograph of graphene sheet protruding from a composite fracture surface. C) Representative stress-strain curves of PET and PET:Graphene-0.07%. D) SEM image of the surface of a vacuum filtered graphene film. E) Sheet resistance versus thickness for as-made and annealed SEG films. The black and red lines illustrate the behaviour expected from films with conductivities 200 and 400 S/m respectively. F) J-V curves for dye-sensitised solar cells with an ITO/Pt counter electrode (black) and a mixer-exfoliated graphene electrode (red). G) Areal capacitance versus frequency for a 25 nm thick graphene electrode prepared in this work. H) Capacitance per unit area, measured at 120 Hz *versus* impedance phase angle for a 25 nm thick graphene electrode prepared in this work, a 600 nm thick graphene electrode described in ref [37], a

commercial capacitive filter[35] and a dielectric capacitor with nanotube electrodes[36]. I) Applied strain and J) measured resistance as a function of time for an elastomer/graphene composite strain sensor.

Supplementary Materials: All is combined as a separate file

References and Notes:

1 Novoselov, K. S. *et al.* A roadmap for graphene. *Nature* **490**, 192-200, (2012).
2 Kavan, L., Yum, J. H. & Gratzel, M. Optically Transparent Cathode for Dye-Sensitized Solar Cells Based on Graphene Nanoplatelets. *Acs Nano* **5**, 165-172, (2011).
3 Pumera, M. Electrochemistry of Graphene: New Horizons for Sensing and Energy Storage. *Chemical Record* **9**, 211-223, (2009).
4 Keeley, G. P. *et al.* Electrochemical ascorbic acid sensor based on DMF-exfoliated graphene. *Journal of Materials Chemistry* **20**, 7864-7869, (2010).
5 Nicolosi, N., Chhowalla, M., Kanatzidis, M. G., Strano, M. S. & Coleman, J. N. Liquid exfoliation of layered materials. *Science* **340**, 1420, (2013).
6 Park, S. & Ruoff, R. S. Chemical methods for the production of graphenes. *Nature Nanotechnology* **4**, 217-224, (2009).
7 Stankovich, S. *et al.* Synthesis of graphene-based nanosheets via chemical reduction of exfoliated graphite oxide. *Carbon* **45**, 1558-1565, (2007).
8 Allen, M. J., Tung, V. C. & Kaner, R. B. Honeycomb Carbon: A Review of Graphene. *Chemical Reviews* **110**, 132-145, (2010).
9 Zhu, Y. W. *et al.* Graphene and Graphene Oxide: Synthesis, Properties, and Applications. *Advanced Materials* **22**, 3906-3924, (2010).
10 Hernandez, Y. *et al.* High-yield production of graphene by liquid-phase exfoliation of graphite. *Nature Nanotechnology* **3**, 563-568, (2008).
11 Coleman, J. N. *et al.* Two-Dimensional Nanosheets Produced by Liquid Exfoliation of Layered Materials. *Science* **331**, 568-571, (2011).
12 Lotya, M. *et al.* Liquid Phase Production of Graphene by Exfoliation of Graphite in Surfactant/Water Solutions. *Journal of the American Chemical Society* **131**, 3611-3620, (2009).
13 Smith, R. J. *et al.* Large-Scale Exfoliation of Inorganic Layered Compounds in Aqueous Surfactant Solutions. *Advanced Materials* **23**, 3944-+, (2011).
14 *See online supporting information*.
15 Wengeler, R. & Nirschl, H. Turbulent hydrodynamic stress induced dispersion and fragmentation of nanoscale agglomerates. *Journal of Colloid and Interface Science* **306**, 262-273, (2007).
16 Murphy, D. W. & Hull, G. W. Monodispersed Tantalum DiSulfide and Adsorption Complexes with Cations. *Journal of Chemical Physics* **62**, 973-978, (1975).
17 Walker, G. F. & Garrett, W. G. Chemical Exfoliation of Vermiculite and Production of Colloidal Dispersions. *Science* **156**, 385-&, (1967).
18 Bunnell, L. R. Method for producing thin graphite flakes with large aspect ratios. USA patent (1993).
19 Guo, J. Low-temperature method of producing nano-scaled graphene platelets and their nanocomposites. USA patent (2012).
20 Holland, F. A. & Chapman, F. S. *Liquid mixing and processing in stirred tanks*. (Reinhold Pub. Corp, 1966).
21 Khan, U. *et al.* Solvent-Exfoliated Graphene at Extremely High Concentration. *Langmuir* **27**, 9077-9082, (2011).

22 Chen, X. J., Dobson, J. F. & Raston, C. L. Vortex fluidic exfoliation of graphite and boron nitride. *Chemical Communications* **48**, 3703-3705, (2012).
23 Khan, U., O'Neill, A., Lotya, M., De, S. & Coleman, J. N. High-Concentration Solvent Exfoliation of Graphene. *Small* **6**, 864-871, (2010).
24 Eckmann, A. *et al.* Probing the Nature of Defects in Graphene by Raman Spectroscopy. *Nano Letters* **12**, 3925-3930, (2012).
25 Kresta, S. M. & Brodkey, R. S. in *Handbook of Industrial Mixing: Science and Practice* (eds E.L. Paul, V.A. Atiemo-Obeng, & S.M. Kresta) 19-87 (John Wiley & Sons, Inc, 2004).
26 Alhassan, S. M., Qutubuddin, S. & Schiraldi, D. A. Graphene Arrested in Laponite-Water Colloidal Glass. *Langmuir* **28**, 4009-4015, (2012).
27 Utomo, A. T., Baker, M. & Pacek, A. W. Flow pattern, periodicity and energy dissipation in a batch rotor-stator mixer. *Chemical Engineering Research & Design* **86**, 1397-1409, (2008).
28 Gollub, J. P. & Swinney, H. L. Onset of Turbulencein a Rotating Fluid. *Physical Review Letters* **35**, 927-930, (1975).
29 Hall, S., Cooke, M., Pacek, A. W., Kowalski, A. J. & Rothman, D. Scaling up of silverson rotor-stator mixers. *Canadian Journal of Chemical Engineering* **89**, 1040-1050, (2011).
30 Leng, D. E. & Calabrese, R. V. in *Handbook of Industrial Mixing: Science and Practice* (eds E.L. Paul, V.A. Atiemo-Obeng, & S.M. Kresta) 639–753 (John Wiley and Sons, 2004).
31 Doran, P. M. *Bioprocess Engineering Principles*. (Academic Press, 1995).
32 Ozcan-Taskin, N. G., Padron, G. & Voelkel, A. Effect of particle type on the mechanisms of break up of nanoscale particle clusters. *Chemical Engineering Research & Design* **87**, 468-473, (2009).
33 Pohl, M. & Schubert, H. in *Partec 2004* 1-4 (2004).
34 De, S. & Coleman, J. N. Are There Fundamental Limitations on the Sheet Resistance and Transmittance of Thin Graphene Films? *Acs Nano* **4**, 2713-2720, (2010).
35 Lin, J. *et al.* 3-Dimensional Graphene Carbon Nanotube Carpet-Based Microsupercapacitors with High Electrochemical Performance. *Nano Letters* **13**, 72-78, (2013).
36 Sorel, S., Khan, U. & Coleman, J. N. Flexible, transparent dielectric capacitors with nanostructured electrodes. *Applied Physics Letters* **101**, 103106, (2012).
37 Miller, J. R., Outlaw, R. A. & Holloway, B. C. Graphene Double-Layer Capacitor with ac Line-Filtering Performance. *Science* **329**, 1637-1639, (2010).
38 Li, X. *et al.* Stretchable and highly sensitive graphene-on-polymer strain sensors. *Scientific Reports* **2**, 870, (2012).